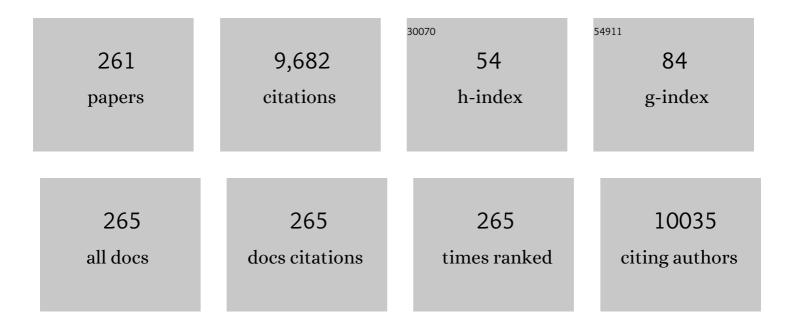
Zhaoxin Wu

List of Publications by Year in descending order

Source: https://exaly.com/author-pdf/1867766/publications.pdf Version: 2024-02-01



#	Article	IF	CITATIONS
1	Stabilizing black-phase formamidinium perovskite formation at room temperature and high humidity. Science, 2021, 371, 1359-1364.	12.6	508
2	Defects in metal triiodide perovskite materials towards high-performance solar cells: origin, impact, characterization, and engineering. Chemical Society Reviews, 2018, 47, 4581-4610.	38.1	455
3	Highâ€Quality Cs ₂ AgBiBr ₆ Double Perovskite Film for Leadâ€Free Inverted Planar Heterojunction Solar Cells with 2.2 % Efficiency. ChemPhysChem, 2018, 19, 1696-1700.	2.1	306
4	Bilateral Interface Engineering toward Efficient 2D–3D Bulk Heterojunction Tin Halide Lead-Free Perovskite Solar Cells. ACS Energy Letters, 2018, 3, 713-721.	17.4	191
5	Conjugated Organic Cations Enable Efficient Self-Healing FASnI3 Solar Cells. Joule, 2019, 3, 3072-3087.	24.0	190
6	Solvent Engineering of the Precursor Solution toward Largeâ€Area Production of Perovskite Solar Cells. Advanced Materials, 2021, 33, e2005410.	21.0	182
7	Improved light absorption and charge transport for perovskite solar cells with rough interfaces by sequential deposition. Nanoscale, 2014, 6, 8171-8176.	5.6	172
8	Construction of Compact Methylammonium Bismuth Iodide Film Promoting Lead-Free Inverted Planar Heterojunction Organohalide Solar Cells with Open-Circuit Voltage over 0.8 V. Journal of Physical Chemistry Letters, 2017, 8, 394-400.	4.6	151
9	A Strategy for Architecture Design of Crystalline Perovskite Lightâ€Emitting Diodes with High Performance. Advanced Materials, 2018, 30, e1800251.	21.0	148
10	Facile one-pot synthesis of MoS ₂ quantum dots–graphene–TiO ₂ composites for highly enhanced photocatalytic properties. Chemical Communications, 2015, 51, 1709-1712.	4.1	144
11	Measurement of the collision time of dense electronic plasma induced by a femtosecond laser in fused silica. Optics Letters, 2005, 30, 320.	3.3	138
12	Multichannel Interdiffusion Driven FASnI ₃ Film Formation Using Aqueous Hybrid Salt/Polymer Solutions toward Flexible Leadâ€Free Perovskite Solar Cells. Advanced Materials, 2017, 29, 1606964.	21.0	137
13	Charge Transport between Coupling Colloidal Perovskite Quantum Dots Assisted by Functional Conjugated Ligands. Angewandte Chemie - International Edition, 2018, 57, 5754-5758.	13.8	117
14	Robust Stability of Efficient Lead-Free Formamidinium Tin Iodide Perovskite Solar Cells Realized by Structural Regulation. Journal of Physical Chemistry Letters, 2018, 9, 6999-7006.	4.6	117
15	Management of perovskite intermediates for highly efficient inverted planar heterojunction perovskite solar cells. Journal of Materials Chemistry A, 2017, 5, 3193-3202.	10.3	113
16	Pseudohalideâ€Induced Recrystallization Engineering for CH ₃ NH ₃ PbI ₃ Film and Its Application in Highly Efficient Inverted Planar Heterojunction Perovskite Solar Cells. Advanced Functional Materials, 2018, 28, 1704836.	14.9	112
17	A Flexible and Thin Graphene/Silver Nanowires/Polymer Hybrid Transparent Electrode for Optoelectronic Devices. ACS Applied Materials & Interfaces, 2016, 8, 31212-31221.	8.0	105
18	One-pot synthesis of Ag/r-GO/TiO2 nanocomposites with high solar absorption and enhanced anti-recombination in photocatalytic applications. Nanoscale, 2014, 6, 5498.	5.6	102

#	Article	IF	CITATIONS
19	Flexible Perovskite Solar Cells with High Power-Per-Weight: Progress, Application, and Perspectives. ACS Energy Letters, 2021, 6, 2917-2943.	17.4	100
20	Graphitic carbon nitride doped SnO ₂ enabling efficient perovskite solar cells with PCEs exceeding 22%. Journal of Materials Chemistry A, 2020, 8, 2644-2653.	10.3	98
21	Ligand Orientation-Induced Lattice Robustness for Highly Efficient and Stable Tin-Based Perovskite Solar Cells. ACS Energy Letters, 2020, 5, 2327-2334.	17.4	98
22	lonic Liquids-Enabled Efficient and Stable Perovskite Photovoltaics: Progress and Challenges. ACS Energy Letters, 0, , 1453-1479.	17.4	98
23	Polarization‣ensitive Halide Perovskites for Polarized Luminescence and Detection: Recent Advances and Perspectives. Advanced Materials, 2021, 33, e2003615.	21.0	89
24	Conjugated Molecules "Bridge― Functional Ligand toward Highly Efficient and Longâ€Term Stable Perovskite Solar Cell. Advanced Functional Materials, 2019, 29, 1808119.	14.9	88
25	A highly efficient mesoscopic solar cell based on CH ₃ NH ₃ PbI _{3â^'x} Cl _x fabricated via sequential solution deposition. Chemical Communications, 2014, 50, 12458-12461.	4.1	87
26	Alternative Organic Spacers for More Efficient Perovskite Solar Cells Containing Ruddlesden–Popper Phases. Journal of the American Chemical Society, 2020, 142, 19705-19714.	13.7	83
27	A‣ite Cation Engineering of Metal Halide Perovskites: Version 3.0 of Efficient Tinâ€Based Leadâ€Free Perovskite Solar Cells. Advanced Functional Materials, 2020, 30, 2000794.	14.9	81
28	A Cocktail of Multiple Cations in Inorganic Halide Perovskite toward Efficient and Highly Stable Blue Light-Emitting Diodes. ACS Energy Letters, 2020, 5, 1062-1069.	17.4	79
29	Enhancing Molecular Aggregations by Intermolecular Hydrogen Bonds to Develop Phosphorescent Emitters for Highâ€Performance Nearâ€Infrared OLEDs. Advanced Science, 2019, 6, 1801930.	11.2	78
30	Multiple foci and a long filament observed with focused femtosecond pulse propagation in fused silica. Optics Letters, 2002, 27, 448.	3.3	76
31	Diarylboronâ€Based Asymmetric Redâ€Emitting Ir(III) Complex for Solutionâ€Processed Phosphorescent Organic Lightâ€Emitting Diode with External Quantum Efficiency above 28%. Advanced Science, 2018, 5, 1701067.	11.2	76
32	One-Step Co-Evaporation of All-Inorganic Perovskite Thin Films with Room-Temperature Ultralow Amplified Spontaneous Emission Threshold and Air Stability. ACS Applied Materials & Interfaces, 2018, 10, 40661-40671.	8.0	76
33	Suppressing Ion Migration Enables Stable Perovskite Lightâ€Emitting Diodes with Allâ€Inorganic Strategy. Advanced Functional Materials, 2020, 30, 2001834.	14.9	76
34	Architecture of p-i-n Sn-Based Perovskite Solar Cells: Characteristics, Advances, and Perspectives. ACS Energy Letters, 2021, 6, 2863-2875.	17.4	76
35	Optics–electrics highways: Plasmonic silver nanowires@TiO2 core–shell nanocomposites for enhanced dye-sensitized solar cells performance. Nano Energy, 2014, 10, 181-191.	16.0	67
36	<i>In Situ</i> Interface Engineering for Highly Efficient Electron-Transport-Layer-Free Perovskite Solar Cells. Nano Letters, 2020, 20, 5799-5806.	9.1	67

#	Article	IF	CITATIONS
37	Study on Photoluminescence Quenching and Photostability Enhancement of MEH-PPV by Reduced Graphene Oxide. Journal of Physical Chemistry C, 2012, 116, 23053-23060.	3.1	65
38	Ag-encapsulated Au plasmonic nanorods for enhanced dye-sensitized solar cell performance. Journal of Materials Chemistry A, 2015, 3, 4659-4668.	10.3	65
39	The role of reduction extent of graphene oxide in the photocatalytic performance of Ag/AgX (X = Cl,) Tj ETQq1 Physical Chemistry Chemical Physics, 2016, 18, 18219-18226.	1 0.784314 2.8	4 rgBT /Over 65
40	Chemical sintering reduced grain boundary defects for stable planar perovskite solar cells. Nano Energy, 2019, 56, 741-750.	16.0	65
41	Thiazole-based metallophosphors of iridium with balanced carrier injection/transporting features and their two-colour WOLEDs fabricated by both vacuum deposition and solution processing-vacuum deposition hybrid strategy. Journal of Materials Chemistry, 2012, 22, 7136.	6.7	64
42	Cyclometalated Platinum Complexes with Aggregation-Induced Phosphorescence Emission Behavior and Highly Efficient Electroluminescent Ability. Chemistry of Materials, 2018, 30, 929-946.	6.7	64
43	Crystallization Dynamics of Snâ€Based Perovskite Thin Films: Toward Efficient and Stable Photovoltaic Devices. Advanced Energy Materials, 2022, 12, 2102213.	19.5	63
44	Highly Transparent, Conductive, Flexible Resin Films Embedded with Silver Nanowires. Langmuir, 2015, 31, 4950-4957.	3.5	62
45	Flexible and Transparent Ferroferric Oxide-Modified Silver Nanowire Film for Efficient Electromagnetic Interference Shielding. ACS Applied Materials & Interfaces, 2020, 12, 2826-2834.	8.0	62
46	Formation of ultrasmooth perovskite films toward highly efficient inverted planar heterojunction solar cells by micro-flowing anti-solvent deposition in air. Journal of Materials Chemistry A, 2016, 4, 6295-6303.	10.3	61
47	High-Brightness and Color-Tunable FAPbBr ₃ Perovskite Nanocrystals 2.0 Enable Ultrapure Green Luminescence for Achieving Recommendation 2020 Displays. ACS Applied Materials & Interfaces, 2020, 12, 2835-2841.	8.0	61
48	Origin of High Efficiency and Long-Term Stability in Ionic Liquid Perovskite Photovoltaic. Research, 2020, 2016345.	5.7	59
49	Asymmetric <i>tris</i> -Heteroleptic Iridium ^{III} Complexes Containing a 9-Phenyl-9-phosphafluorene Oxide Moiety with Enhanced Charge Carrier Injection/Transporting Properties for Highly Efficient Solution-Processed Organic Light-Emitting Diodes. Chemistry of Materials. 2016. 28, 8556-8569.	6.7	58
50	Rubidium Doping for Enhanced Performance of Highly Efficient Formamidinium-Based Perovskite Light-Emitting Diodes. ACS Applied Materials & Interfaces, 2018, 10, 9849-9857.	8.0	58
51	Asymmetric thermally activated delayed fluorescence (TADF) emitters with 5,9-dioxa-13 <i>b</i> -boranaphtho[3,2,1- <i>de</i>]anthracene (OBA) as the acceptor and highly efficient blue-emitting OLEDs. Journal of Materials Chemistry C, 2019, 7, 11953-11963.	5.5	58
52	Multifunctional perovskite capping layers in hybrid solar cells. Journal of Materials Chemistry A, 2014, 2, 14973.	10.3	57
53	Phosphorescent Iridium(III) Complexes Bearing Fluorinated Aromatic Sulfonyl Group with Nearly Unity Phosphorescent Quantum Yields and Outstanding Electroluminescent Properties. ACS Applied Materials & Interfaces, 2015, 7, 24703-24714.	8.0	57
54	Surface mediated ligands addressing bottleneck of room-temperature synthesized inorganic perovskite nanocrystals toward efficient light-emitting diodes. Nano Energy, 2020, 70, 104467.	16.0	56

#	Article	IF	CITATIONS
55	Investigation of the spectra of phosphorescent organic light-emitting devices in relation to emission zone. Journal of Applied Physics, 2005, 97, 103105.	2.5	55
56	Highly efficient deep-blue organic electroluminescent devices (CIEy â‰^ 0.08) doped with fluorinated 9,9′-bianthracene derivatives (fluorophores). Journal of Materials Chemistry C, 2013, 1, 8117.	5.5	55
57	One-Step Preparation and Assembly of Aqueous Colloidal CdS _{<i>x</i>} Se _{1–<i>x</i>} Nanocrystals within Mesoporous TiO ₂ Films for Quantum Dot-Sensitized Solar Cells. ACS Applied Materials & Interfaces, 2013, 5, 5139-5148.	8.0	55
58	Highly Strain and Bending Sensitive Microtapered Long-Period Fiber Gratings. IEEE Photonics Technology Letters, 2017, 29, 1085-1088.	2.5	53
59	Rational Core–Shell Design of Open Air Low Temperature In Situ Processable CsPbI ₃ Quasiâ€Nanocrystals for Stabilized pâ€iâ€n Solar Cells. Advanced Energy Materials, 2019, 9, 1901787.	19.5	53
60	Highly efficient and stable perovskite solar cells enabled by low-dimensional perovskitoids. Science Advances, 2022, 8, eabk2722.	10.3	53
61	Highly Efficient Deep-Red Organic Light-Emitting Devices Based on Asymmetric Iridium(III) Complexes with the Thianthrene 5,5,10,10-Tetraoxide Moiety. ACS Applied Materials & Interfaces, 2019, 11, 26152-26164.	8.0	52
62	Fluorinated 9,9′-spirobifluorene derivatives as host materials for highly efficient blue organic light-emitting devices. Journal of Materials Chemistry C, 2013, 1, 2183.	5.5	51
63	High Stability and Ultralow Threshold Amplified Spontaneous Emission from Formamidinium Lead Halide Perovskite Films. Journal of Physical Chemistry C, 2017, 121, 15318-15325.	3.1	50
64	Ultra-stable CsPbBr ₃ nanocrystals with near-unity photoluminescence quantum yield <i>via</i> postsynthetic surface engineering. Journal of Materials Chemistry A, 2019, 7, 26116-26122.	10.3	50
65	Vacuum Dual-Source Thermal-Deposited Lead-Free Cs ₃ Cu ₂ I ₅ Films with High Photoluminescence Quantum Yield for Deep-Blue Light-Emitting Diodes. ACS Applied Materials & Interfaces, 2020, 12, 52967-52975.	8.0	50
66	Filamentation and temporal reshaping of a femtosecond pulse in fused silica. Physical Review A, 2003, 68, .	2.5	49
67	Novel iridium(<scp>iii</scp>) complexes bearing dimesitylboron groups with nearly 100% phosphorescent quantum yields for highly efficient organic light-emitting diodes. Journal of Materials Chemistry C, 2017, 5, 7871-7883.	5.5	49
68	Versatile Fluorinated Derivatives of Triphenylamine as Hole-Transporters and Blue-Violet Emitters in Organic Light-Emitting Devices. Journal of Physical Chemistry C, 2012, 116, 20504-20512.	3.1	47
69	Allâ€Inorganic Heteroâ€Structured Cesium Tin Halide Perovskite Lightâ€Emitting Diodes With Current Density Over 900 A cm ^{â^2} and Its Amplified Spontaneous Emission Behaviors. Physica Sta Solidi - Rapid Research Letters, 2018, 12, 1800090.	itu 3. 4	47
70	Stability Improvement of Tinâ€Based Halide Perovskite by Precursorâ€Solution Regulation with Dualâ€Functional Reagents. Advanced Functional Materials, 2021, 31, 2104344.	14.9	47
71	Facet-Dependent Control of PbI ₂ Colloids for over 20% Efficient Perovskite Solar Cells. ACS Energy Letters, 2019, 4, 358-367.	17.4	46
72	A comparison study between ZnO nanorods coated with graphene oxide and reduced graphene oxide. Journal of Alloys and Compounds, 2014, 582, 29-32.	5.5	44

#	Article	IF	CITATIONS
73	Effective blocking of the molecular aggregation of novel truxene-based emitters with spirobifluorene and electron-donating moieties for furnishing highly efficient non-doped blue-emitting OLEDs. Journal of Materials Chemistry C, 2015, 3, 5783-5794.	5.5	41
74	Online fabrication scheme of helical long-period fiber grating for liquid-level sensing. Applied Optics, 2016, 55, 9675.	2.1	41
75	A facile one-step solution deposition via non-solvent/solvent mixture for efficient organometal halide perovskite light-emitting diodes. Nanoscale, 2016, 8, 11084-11090.	5.6	41
76	Solution-processed organic films of multiple small-molecules and white light-emitting diodes. Organic Electronics, 2010, 11, 641-648.	2.6	38
77	Random lasing from granular surface of waveguide with blends of PS and PMMA. Optics Express, 2011, 19, 16126.	3.4	37
78	Highly-efficient and low-temperature perovskite solar cells by employing a Bi-hole transport layer consisting of vanadium oxide and copper phthalocyanine. Chemical Communications, 2018, 54, 6177-6180.	4.1	37
79	Improvement of light extraction in organic light-emitting diodes using a corrugated microcavity. Optics Express, 2015, 23, 4055.	3.4	36
80	Stability of Sn-Pb mixed organic–inorganic halide perovskite solar cells: Progress, challenges, and perspectives. Journal of Energy Chemistry, 2022, 65, 371-404.	12.9	36
81	Considerable improvement in the stability of solution processed small molecule OLED by annealing. Applied Surface Science, 2011, 257, 7394-7398.	6.1	35
82	Initiating crystal growth kinetics of α-HC(NH2)2PbI3 for flexible solar cells with long-term stability. Nano Energy, 2016, 26, 438-445.	16.0	35
83	Organic Emitters with a Rigid 9-Phenyl-9-phosphafluorene Oxide Moiety as the Acceptor and Their Thermally Activated Delayed Fluorescence Behavior. ACS Applied Materials & Interfaces, 2019, 11, 27112-27124.	8.0	35
84	Postâ€Treatment Engineering of Vacuumâ€Deposited Cs ₂ NaBil ₆ Double Perovskite Film for Enhanced Photovoltaic Performance. Physica Status Solidi (A) Applications and Materials Science, 2019, 216, 1900567.	1.8	35
85	Allâ€inorganic Snâ€based Perovskite Solar Cells: Status, Challenges, and Perspectives. ChemSusChem, 2020, 13, 6477-6497.	6.8	35
86	Piperidine-induced Switching of the direct band gaps of Ag(<scp>i</scp>)/Bi(<scp>iii</scp>) bimetallic iodide double perovskites. Journal of Materials Chemistry C, 2020, 8, 5349-5354.	5.5	34
87	Alcohol-assisted photoetching of silicon carbide with a femtosecond laser. Optics Communications, 2009, 282, 78-80.	2.1	33
88	Template effects in Cu(<scp>i</scp>)–Bi(<scp>iii</scp>) iodide double perovskites: a study of crystal structure, film orientation, band gap and photocurrent response. Journal of Materials Chemistry A, 2020, 8, 7288-7296.	10.3	33
89	Strain Engineering of Metal–Halide Perovskites toward Efficient Photovoltaics: Advances and Perspectives. Solar Rrl, 2021, 5, 2000672.	5.8	33
90	Enhance the responsivity and response speed of self-powered ultraviolet photodetector by GaN/CsPbBr3 core-shell nanowire heterojunction and hydrogel. Nano Energy, 2022, 100, 107437.	16.0	33

#	Article	IF	CITATIONS
91	Morphological investigation at the front and rear surfaces of fused silica processed with femtosecond laser pulses in air. Optics Express, 2002, 10, 1244.	3.4	32
92	Plasmonic enhancement for high efficient and stable perovskite solar cells by employing "hot spots" Au nanobipyramids. Organic Electronics, 2018, 60, 1-8.	2.6	32
93	Interface Engineering in Tin Perovskite Solar Cells. Advanced Materials Interfaces, 2019, 6, 1901322.	3.7	32
94	Photoinduced Cross Linkable Polymerization of Flexible Perovskite Solar Cells and Modules by Incorporating Benzyl Acrylate. Advanced Functional Materials, 2022, 32, .	14.9	32
95	Highly efficient electroluminescent Pt ^{II} ppy-type complexes with monodentate ligands. Chemical Communications, 2017, 53, 7581-7584.	4.1	31
96	One-dimensional (1D) [6,6]-phenyl-C ₆₁ -butyric acid methyl ester (PCBM) nanorods as an efficient additive for improving the efficiency and stability of perovskite solar cells. Journal of Materials Chemistry A, 2016, 4, 8566-8572.	10.3	30
97	Aggregation-induced emission triggered by the radiative-transition-switch of a cyclometallated Pt(<scp>ii</scp>) complex. Journal of Materials Chemistry C, 2019, 7, 12552-12559.	5.5	30
98	Morphologically controlled electrodeposition of CdSe on mesoporous TiO2 film for quantum dot-sensitized solar cells. Electrochimica Acta, 2013, 108, 449-457.	5.2	29
99	Bifunctional π-conjugated ligand assisted stable and efficient perovskite solar cell fabrication <i>via</i> interfacial stitching. Journal of Materials Chemistry A, 2019, 7, 16533-16540.	10.3	29
100	Flexible Perovskite Solar Modules with Functional Layers Fully Vacuum Deposited. Solar Rrl, 2020, 4, 2000292.	5.8	29
101	Simple Tuning of the Optoelectronic Properties of Ir ^{III} and Pt ^{II} Electrophosphors Based on Linkage Isomer Formation with a Naphthylthiazolyl Moiety. European Journal of Inorganic Chemistry, 2012, 2012, 2278-2288.	2.0	28
102	Modified deposition process of electron transport layer for efficient inverted planar perovskite solar cells. Chemical Communications, 2015, 51, 8986-8989.	4.1	28
103	The enhanced random lasing from dye-doped polymer films with different-sized silver nanoparticles. Organic Electronics, 2016, 30, 165-170.	2.6	28
104	Bis-Zn ^{II} salphen complexes bearing pyridyl functionalized ligands for efficient organic light-emitting diodes (OLEDs). Dalton Transactions, 2017, 46, 6098-6110.	3.3	28
105	Real-time image haze removal using an aperture-division polarimetric camera. Applied Optics, 2017, 56, 942.	2.1	28
106	A robust haze-removal scheme in polarimetric dehazing imaging based on automatic identification of sky region. Optics and Laser Technology, 2016, 86, 145-151.	4.6	27
107	High Triplet Energy Level Achieved by Tuning the Arrangement of Building Blocks in Phosphorescent Polymer Backbones for Furnishing High Electroluminescent Performances in Both Blue and White Organic Light-Emitting Devices. ACS Applied Materials & Interfaces, 2017, 9, 16360-16374.	8.0	27
108	A general route to enhance the fluorescence of graphene quantum dots by Ag nanoparticles. RSC Advances, 2014, 4, 21772-21776.	3.6	26

#	Article	IF	CITATIONS
109	Strategically Formulating Aggregationâ€Induced Emissionâ€Active Phosphorescent Emitters by Restricting the Coordination Skeletal Deformation of Pt(II) Complexes Containing Two Independent Monodentate Ligands. Advanced Optical Materials, 2020, 8, 2000079.	7.3	26
110	Contrast-enhancement in organic light-emitting diodes. Optics Express, 2005, 13, 1406.	3.4	25
111	Efficient and Stable Perovskite Solar Cells by Fluorinated Ionic Liquid–Induced Component Interaction. Solar Rrl, 2021, 5, .	5.8	24
112	Abnormal spatial heterogeneity governing the charge-carrier mechanism in efficient Ruddlesden–Popper perovskite solar cells. Energy and Environmental Science, 2021, 14, 4915-4925.	30.8	24
113	Aggregation-induced phosphorescence emission (AIPE) behaviors in Pt ^{II} (C^N)(N-donor) Tj ETQq1 1 C skeleton and their optoelectronic properties. Journal of Materials Chemistry C, 2021, 9, 2334-2349.).784314 ı 5.5	gBT /Over 24
114	A hybrid encapsulation of organic light-emitting devices. Journal Physics D: Applied Physics, 2005, 38, 981-984.	2.8	23
115	Iridium (III) complexes with 5,5-dimethyl-3-(pyridin-2-yl)cyclohex-2-enone ligands as sensitizer for dye-sensitized solar cells. Organic Electronics, 2013, 14, 3297-3305.	2.6	23
116	Fluorinated 9,9′-bianthracene derivatives with twisted intramolecular charge-transfer excited states as blue host materials for high-performance fluorescent electroluminescence. Journal of Materials Chemistry C, 2014, 2, 9375-9384.	5.5	23
117	Asymmetric tris-heteroleptic iridium(<scp>iii</scp>) complexes containing three different 2-phenylpyridine-type ligands: a new strategy for improving the electroluminescence ability of phosphorescent emitters. Journal of Materials Chemistry C, 2018, 6, 9453-9464.	5.5	23
118	Isomers of Coumarin-Based Cyclometalated Ir(III) Complexes with Easily Tuned Phosphorescent Color and Features for Highly Efficient Organic Light-Emitting Diodes. Inorganic Chemistry, 2019, 58, 7393-7408.	4.0	23
119	Near-unity blue luminance from lead-free copper halides for light-emitting diodes. Nano Energy, 2022, 91, 106664.	16.0	23
120	Charge tunneling injection through a thin teflon film between the electrodes and organic semiconductor layer: Relation to morphology of the teflon film. Physical Review B, 2006, 74, .	3.2	22
121	Novel 2,4-difluorophenyl-functionalized arylamine as hole-injecting/hole-transporting layers in organic light-emitting devices. Chemical Physics Letters, 2012, 527, 36-41.	2.6	22
122	Photoluminescence investigation about zinc oxide with graphene oxide & reduced graphene oxide buffer layers. Journal of Colloid and Interface Science, 2014, 416, 289-293.	9.4	22
123	Formamidine Acetate Induces Regulation of Crystallization and Stabilization in Sn-Based Perovskite Solar Cells. ACS Applied Materials & amp; Interfaces, 2021, 13, 33218-33225.	8.0	22
124	Tris(cyclometalated) Iridium(III) Phosphorescent Complexes with 2â€Phenylthiazoleâ€Type Ligands: Synthesis, Photophysical, Redox and Electrophosphorescent Behavior. European Journal of Inorganic Chemistry, 2013, 2013, 4754-4763.	2.0	21
125	Fluorinated anthracene derivatives as deep-blue emitters and host materials for highly efficient organic light-emitting devices. RSC Advances, 2015, 5, 59027-59036.	3.6	21
126	Controlled thickness and morphology for highly efficient inverted planar heterojunction perovskite solar cells. Nanoscale, 2015, 7, 10699-10707.	5.6	21

#	Article	IF	CITATIONS
127	Homoleptic thiazole-based Ir ^{III} phosphorescent complexes for achieving both high EL efficiencies and an optimized trade-off among the key parameters of solution-processed WOLEDs. Journal of Materials Chemistry C, 2017, 5, 208-219.	5.5	21
128	Lead Sources in Perovskite Solar Cells: Toward Controllable, Sustainable, and Largeâ€Scalable Production. Solar Rrl, 2021, 5, 2100665.	5.8	21
129	Field emission mechanism insights of graphene decorated with ZnO nanoparticles. RSC Advances, 2013, 3, 14073.	3.6	20
130	Platinum(ii) polymetallayne-based phosphorescent polymers with enhanced triplet energy-transfer: synthesis, photophysical, electrochemistry, and electrophosphorescent investigation. RSC Advances, 2015, 5, 36507-36519.	3.6	20
131	Charged dinuclear Cu(I) complexes for solution-processed single-emitter warm white organic light-emitting devices. Dyes and Pigments, 2017, 143, 151-164.	3.7	20
132	High performance organo-lead halide perovskite light-emitting diodes via surface passivation of phenethylamine. Organic Electronics, 2018, 60, 57-63.	2.6	20
133	Asymmetric Heteroleptic Ir(III) Phosphorescent Complexes with Aromatic Selenide and Selenophene Groups: Synthesis and Photophysical, Electrochemical, and Electrophosphorescent Behaviors. Inorganic Chemistry, 2018, 57, 11027-11043.	4.0	20
134	Towards high performance solution-processed orange organic light-emitting devices: precisely-adjusting properties of Ir(<scp>iii</scp>) complexes by reasonably engineering the asymmetric configuration with second functionalized cyclometalating ligands. Journal of Materials Chemistry C, 2019, 7, 8836-8846.	5.5	20
135	Emerging Organic/Hybrid Photovoltaic Cells for Indoor Applications: Recent Advances and Perspectives. Solar Rrl, 2021, 5, 2100042.	5.8	20
136	Surface-tension release in PTAA-based inverted perovskite solar cells. Organic Electronics, 2022, 100, 106378.	2.6	20
137	Theoretical insight into the deep-blue amplified spontaneous emission of new organic semiconductor molecules. Organic Electronics, 2014, 15, 3144-3153.	2.6	19
138	A nanostructure-based counter electrode for dye-sensitized solar cells by assembly of silver nanoparticles. Organic Electronics, 2014, 15, 1641-1649.	2.6	19
139	Electric field-modulated amplified spontaneous emission in organo-lead halide perovskite CH3NH3PbI3. Applied Physics Letters, 2015, 107, .	3.3	19
140	Realizing improved performance of down-conversion white organic light-emitting diodes by localized surface plasmon resonance effect of Ag nanoparticles. Organic Electronics, 2016, 31, 234-239.	2.6	19
141	Impermeable inorganic "walls―sandwiching perovskite layer toward inverted and indoor photovoltaic devices. Nano Energy, 2021, 88, 106286.	16.0	19
142	Silver-loaded anatase nanotubes dispersed plasmonic composite photoanode for dye-sensitized solar cells. Organic Electronics, 2014, 15, 2847-2854.	2.6	18
143	A new type of solid-state luminescent 2-phenylbenzo[<i>g</i>]furo[2,3- <i>b</i>]quinoxaline derivative: synthesis, photophysical characterization and transporting properties. Journal of Materials Chemistry C, 2019, 7, 9690-9697.	5.5	18
144	Designing Ionic Liquids as the Solvent for Efficient and Stable Perovskite Solar Cells. ACS Applied Materials & Interfaces, 2022, 14, 22870-22878.	8.0	18

#	Article	IF	CITATIONS
145	Enhancement of amplified spontaneous emission in organic gain media by the metallic film. Organic Electronics, 2014, 15, 2052-2058.	2.6	17
146	Novel phosphorescent polymers containing both ambipolar segments and functionalized Ir ^{III} phosphorescent moieties: synthesis, photophysical, redox, and electrophosphorescence investigation. Journal of Materials Chemistry C, 2014, 2, 9523-9535.	5.5	17
147	The synthesis and mechanism exploration of europium-doped LiYF4 micro-octahedron phosphors with multilevel interiors. Dalton Transactions, 2014, 43, 5453.	3.3	17
148	High Efficiency Fluorescent Electroluminescence with Extremely Low Efficiency Rollâ€Off Generated by a Donor–Bianthracene–Acceptor Structure: Utilizing Perpendicular Twisted Intramolecular Charge Transfer Excited State. Advanced Optical Materials, 2018, 6, 1800060.	7.3	17
149	Strategy for achieving efficient electroluminescence with reduced efficiency roll-off: enhancement of hot excitons spin mixing and restriction of internal conversion by twisted structure regulation using an anthracene derivative. Journal of Materials Chemistry C, 2019, 7, 5604-5614.	5.5	17
150	Wide tuning of emission color of iridium (III) complexes from green to deep red via dicyanovinyl substituent effect on 2-phenylpyridine ligands. Organic Electronics, 2013, 14, 2233-2242.	2.6	16
151	Novel Red Phosphorescent Polymers Bearing Both Ambipolar and Functionalized Ir ^{III} Phosphorescent Moieties for Highly Efficient Organic Light-Emitting Diodes. Macromolecular Rapid Communications, 2015, 36, 71-78.	3.9	16
152	Silver/graphene nanocomposites as catalysts for the reduction of <i>p</i> â€nitrophenol to <i>p</i> â€aminophenol: Materials preparation and reaction kinetics studies. Canadian Journal of Chemical Engineering, 2017, 95, 1297-1304.	1.7	16
153	Chiral cation promoted interfacial charge extraction for efficient tin-based perovskite solar cells. Journal of Energy Chemistry, 2022, 68, 789-796.	12.9	16
154	Structure–Property Relationship of Amplified Spontaneous Emission in Organic Semiconductor Materials: TPD, DPABP, and NPB. Journal of Physical Chemistry A, 2013, 117, 10903-10911.	2.5	15
155	Local nearly non-strained perovskite lattice approaching a broad environmental stability window of efficient solar cells. Nano Energy, 2020, 75, 104940.	16.0	15
156	The refocusing behaviour of a focused femtosecond laser pulse in fused silica. Journal of Optics, 2003, 5, 102-107.	1.5	14
157	Solution-processed white organic light-emitting devices based on small-molecule materials. Journal of Luminescence, 2010, 130, 321-325.	3.1	13
158	Microstructures, surface states and field emission mechanism of graphene–tin/tin oxide hybrids. Journal of Colloid and Interface Science, 2013, 395, 40-44.	9.4	13
159	Effect of fluorocarbon (trifluoromethyl groups) substitution on blue electroluminescent properties of 9,9′-bianthracene derivatives with twisted intramolecular charge-transfer excited states. Dyes and Pigments, 2015, 122, 238-245.	3.7	13
160	Fast polarimetric dehazing method for visibility enhancement in HSI colour space. Journal of Optics (United Kingdom), 2017, 19, 095606.	2.2	13
161	Unsymmetric Heteroleptic Ir(III) Complexes with 2-Phenylquinoline and Coumarin-Based Ligand Isomers for Tuning Character of Triplet Excited States and Achieving High Electroluminescent Efficiencies. Inorganic Chemistry, 2020, 59, 12362-12374.	4.0	13
162	Optimizing molecular rigidity and thermally activated delayed fluorescence (TADF) behavior of phosphoryl center π-conjugated heterocycles-based emitters by tuning chemical features of the tether groups. Chemical Engineering Journal, 2021, 413, 127445.	12.7	13

#	Article	IF	CITATIONS
163	Exciton and bi-exciton mechanisms in amplified spontaneous emission from CsPbBr ₃ perovskite thin films. Optics Express, 2019, 27, 29124.	3.4	13
164	Bi-Linkable Reductive Cation as Molecular Glue for One Year Stable Sn-Based Perovskite Solar Cells. ACS Applied Energy Materials, 2022, 5, 4008-4016.	5.1	13
165	Solution-processed white organic light-emitting diodes with mixed-host structures. Journal of Luminescence, 2012, 132, 697-701.	3.1	12
166	The molecular picture of amplified spontaneous emission of star-shaped functionalized-truxene derivatives. Journal of Materials Chemistry C, 2015, 3, 7004-7013.	5.5	12
167	Enhanced lasing assisted by the Ag-encapsulated Au plasmonic nanorods. Optics Letters, 2015, 40, 990.	3.3	12
168	Efficient Charge Collection Promoted by Interface Passivation Using Amino Acid Toward High Performance Perovskite Solar Cells. Physica Status Solidi - Rapid Research Letters, 2019, 13, 1800505.	2.4	12
169	Self-assembly monomolecular engineering towards efficient and stable inverted perovskite solar cells. Chemical Engineering Journal, 2022, 430, 132986.	12.7	12
170	Improving the stability of organic light-emitting devices using a solution-processed hole-injecting layer. Applied Surface Science, 2009, 255, 7970-7973.	6.1	11
171	Solution-processed p-doped hole-transport layer and its application in organic light-emitting diodes. Applied Surface Science, 2010, 256, 4468-4472.	6.1	11
172	Physical deoxygenation of graphene oxide paper surface and facile in situ synthesis of graphene based ZnO films. Applied Physics Letters, 2014, 105, 233106.	3.3	11
173	Employing the plasmonic effect of the Ag–graphene composite for enhancing light harvesting and photoluminescence quenching efficiency of poly[2-methoxy-5-(2-ethylhexyloxy)-1,4-phenylene-vinylene]. Physical Chemistry Chemical Physics, 2014, 16, 4561.	2.8	11
174	Enhancing the electroluminescence performances of novel platinum(ii) polymetallayne-based phosphorescent polymers through employing functionalized IrIII phosphorescent units and facilitating triplet energy transfer. RSC Advances, 2015, 5, 12100-12110.	3.6	11
175	Facilitating triplet energy-transfer in polymetallayne-based phosphorescent polymers with iridium(III) units and the great potential in achieving high electroluminescent performances. Journal of Organometallic Chemistry, 2015, 794, 1-10.	1.8	11
176	Exploiting a Multiphase Pure Formamidinium Lead Perovskite for Efficient Green-Light-Emitting Diodes. ACS Applied Materials & Interfaces, 2021, 13, 23067-23073.	8.0	11
177	High Triplet Energy Level Molecule Enables Highly Efficient Sky-Blue Perovskite Light-Emitting Diodes. Journal of Physical Chemistry Letters, 2021, 12, 11723-11729.	4.6	11
178	SnO ₂ Passivation and Enhanced Perovskite Charge Extraction with a Benzylamine Hydrochloric Interlayer. ACS Applied Materials & Interfaces, 2022, 14, 34198-34207.	8.0	11
179	Influence of the thickness ofÂN,N′-Bis(naphthalene-1-yl)-N,N′-bis(phenyl) benzidine layer on the performance ofÂorganic light-emitting diodes. Applied Physics A: Materials Science and Processing, 2010, 98, 239-243.	2.3	10
180	Solution-processed small molecule thin films and their light-emitting devices. Thin Solid Films, 2010, 518, 3886-3890.	1.8	10

#	Article	IF	CITATIONS
181	Dependence of the stability of organic light-emitting diodes on driving mode. Science Bulletin, 2011, 56, 2210-2214.	1.7	10
182	Stable amorphous bis(diarylamino)biphenyl derivatives as hole-transporting materials in OLEDs. Electronic Materials Letters, 2013, 9, 655-661.	2.2	10
183	Organic alternating current electroluminescence device based on 4,4′-bis(N-phenyl-1-naphthylamino) biphenyl/1,4,5,8,9,11-hexaazatriphenylene charge generation unit. Organic Electronics, 2015, 17, 44-50.	2.6	10
184	Suppression of efficiency roll-off in TADF-OLEDs using Ag-island nanostructures with localized surface plasmon resonance effect. Organic Electronics, 2017, 51, 173-179.	2.6	10
185	Enhanced lasing from organic gain medium by Au nanocube@SiO ₂ core-shell nanoparticles with optimal size. Optical Materials Express, 2018, 8, 3014.	3.0	10
186	Complementary Triple-Ligand Engineering Approach to Methylamine Lead Bromide Nanocrystals for High-Performance Light-Emitting Diodes. ACS Applied Materials & Interfaces, 2022, 14, 10508-10516.	8.0	10
187	Study on scalable Coulombic degradation for estimating the lifetime of organic light-emitting devices. Journal Physics D: Applied Physics, 2011, 44, 155103.	2.8	9
188	Tunable lasing on silver island films by coupling to the localized surface plasmon. Optical Materials Express, 2015, 5, 629.	3.0	9
189	Efficiency roll-off suppression in organic light-emitting diodes using size-tunable bimetallic bowtie nanoantennas at high current densities. Applied Physics Letters, 2016, 109, .	3.3	9
190	Coordination polymers based on bis-Zn ^{II} salphen complexes and functional ditopic ligands for efficient polymer light-emitting diodes (PLEDs). Polymer Chemistry, 2017, 8, 6368-6377.	3.9	9
191	Unsymmetric 2-phenylpyridine (ppy)-type cyclometalated Ir(<scp>iii</scp>) complexes bearing both 5,9-dioxa-13 <i>b</i> -boranaphtho[3,2,1- <i>de</i>]anthracene and phenylsulfonyl groups for tuning optoelectronic properties and electroluminescence abilities. Inorganic Chemistry Frontiers, 2020, 7, 1651-1666.	6.0	9
192	Antisolventâ€Free Fabrication of Efficient and Stable Sn–Pb Perovskite Solar Cells. Solar Rrl, 2021, 5, 2100675.	5.8	9
193	Manipulating MLCT transition character with ppy-type four-coordinate organoboron skeleton for highly efficient long-wavelength Ir-based phosphors in organic light-emitting diodes. Journal of Materials Chemistry C, 2021, 9, 12650-12660.	5.5	9
194	Different tendencies of breakdown threshold on pulse duration in the subpicosecond regime in fused silica. Journal of Optics, 2005, 7, 198-203.	1.5	8
195	Understanding the growth mechanism of stabilizer-free Ag nanoparticles on reduced graphene oxide: the role of CO. Journal of Nanoparticle Research, 2013, 15, 1.	1.9	8
196	Trifluoromethyl-substituted 9,9'-bianthracene derivative as host material for highly efficient blue OLED. Optical Materials Express, 2015, 5, 2468.	3.0	8
197	Effect of diphenylamine substituent on charge-transfer absorption features of the iridium complexes and application in dye-sensitized solar cell. Journal of Organometallic Chemistry, 2015, 775, 55-59.	1.8	8
198	Enhancement of lasing in organic gain media assisted by the metallic nanoparticles–metallic film plasmonic hybrid structure. Journal of Materials Chemistry C, 2016, 4, 5717-5724.	5.5	8

#	Article	IF	CITATIONS
199	High thermal stability fluorene-based hole-injecting material for organic light-emitting devices. Optical Materials, 2016, 53, 19-23.	3.6	8
200	Single-layer small molecular organic light emitting diodes without hole transport layer. Thin Solid Films, 2009, 517, 3382-3384.	1.8	7
201	Dependence of the organic nonvolatile memory performance on the location of ultra-thin Ag film. Journal Physics D: Applied Physics, 2010, 43, 035101.	2.8	7
202	Sulfide treatment passivation of mid-/long-wave dual-color infrared detectors based on type-II InAs/GaSb superlattices. Optical and Quantum Electronics, 2019, 51, 1.	3.3	7
203	The synthesis of cyclometalated platinum(<scp>ii</scp>) complexes with benzoaryl-pyridines as C^N ligands for investigating their photophysical, electrochemical and electroluminescent properties. Dalton Transactions, 2020, 49, 15633-15645.	3.3	7
204	Optimized trade-off between electroluminescent stability and efficiency in solution-processed WOLEDs adopting functional iridium(III) complexes with 9-phenyl-9-phosphafluorene oxide (PhFIPO) moiety. Organic Electronics, 2020, 84, 105797.	2.6	7
205	Overcoming energy loss of thermally activated delayed fluorescence sensitized-OLEDs by developing a fluorescent dopant with a small singlet–triplet energy splitting. Journal of Materials Chemistry C, 2022, 10, 1681-1689.	5.5	7
206	Micro-ablation at the front and rear surfaces of a fused silica window by using a femtosecond laser pulse in air. Journal of Optics, 2004, 6, 671-674.	1.5	6
207	Silafluorene moieties as promising building blocks for constructing wide-energy-gap host materials of blue phosphorescent organic light-emitting devices. Science China Chemistry, 2015, 58, 993-998.	8.2	6
208	A solvent/non-solvent system for achieving solution-processed multilayer organic light-emitting devices. Thin Solid Films, 2015, 589, 852-856.	1.8	6
209	Efficiency roll-off suppression in organic light-emitting diodes at high current densities using gold bowtie nanoantennas. Applied Physics Express, 2016, 9, 022101.	2.4	6
210	Efficient amplified spontaneous emission based on π-conjugated fluorophore-cored molecules studied by density functional theory. Organic Electronics, 2018, 57, 123-132.	2.6	6
211	Theoretical evidence of low-threshold amplified spontaneous emission in organic emitters: transition density and intramolecular vibrational mode analysis. Physical Chemistry Chemical Physics, 2018, 20, 19515-19524.	2.8	6
212	Inverted with power efficiency over 220ÂlmÂW–1. Nano Energy, 2021, 82, 105660.	16.0	6
213	In Situ Interfacial Passivation of Sn-Based Perovskite Films with a Bi-functional Ionic Salt for Enhanced Photovoltaic Performance. ACS Applied Materials & amp; Interfaces, 2021, , .	8.0	6
214	Unraveling the Role of Chloride in Vertical Growth of Low-Dimensional Ruddlesden–Popper Perovskites for Efficient Perovskite Solar Cells. ACS Applied Materials & Interfaces, 2021, , .	8.0	6
215	Tandem organic light-emitting diodes with an effective nondoped charge-generation unit. Physica Status Solidi (A) Applications and Materials Science, 2013, 210, 2583-2587.	1.8	5
216	Naphthyl-functionalized oligophenyls: Photophysical properties, film morphology, and amplified spontaneous emission. Optical Materials, 2016, 54, 37-44.	3.6	5

#	Article	IF	CITATIONS
217	Perovskite Photovoltaics: Pseudohalideâ€Induced Recrystallization Engineering for CH ₃ NH ₃ Pbl ₃ Film and Its Application in Highly Efficient Inverted Planar Heterojunction Perovskite Solar Cells (Adv. Funct. Mater. 2/2018). Advanced Functional Materials, 2018, 28, 1870013.	14.9	5
218	Heat Dissipation Properties of Thinâ€Film Encapsulation by Insertion of a Metal Thin Film for Organic Lightâ€Emitting Diodes. Physica Status Solidi (A) Applications and Materials Science, 2018, 215, 1800326.	1.8	5
219	Universal polymeric hosts adopting cardo-type backbone prepared by palladium-free catalyst with precisely controlled triplet energy levels and their application for highly efficient solution-processed phosphorescent organic light-emitting devices. Chemical Engineering Journal, 2021. 406. 126717.	12.7	5
220	Enhanced performance of spectra stable blue perovskite light-emitting diodes through Poly(9-vinylcarbazole) interlayer incorporation. Organic Electronics, 2021, 96, 106259.	2.6	5
221	High efficient and stable Tin-based perovskite solar cells via short-chain ligand modification. Organic Electronics, 2021, 96, 106198.	2.6	5
222	Sodium borohydride as an n-type dopant in tris(8-hydroxyquinoline) aluminium thin film. Journal Physics D: Applied Physics, 2009, 42, 205108.	2.8	4
223	Effects of dilution and charge trapping on the performance of a lightâ€emitting diode of poly(9â€vinylcarbazole) doped with poly[2â€methoxyâ€5â€(2′â€ethyl hexyloxy)– 1,4â€phenylene vinylene]. Applied Polymer Science, 2010, 117, 1213-1217.	. Jຂາຍ rnal of	f 4
224	White organic light-emitting devices with a solution-processed small molecular emission layer. Displays, 2012, 33, 129-132.	3.7	4
225	Dicyanovinyl-unit-induced absorption enhancement of iridium(III) complexes in long-wavelength range and potential application in dye-sensitized solar cells. Science China Chemistry, 2015, 58, 658-665.	8.2	4
226	Plasmonically enhanced lasing by different size silver nanoparticles-silver film hybrid structure. Organic Electronics, 2017, 50, 403-410.	2.6	4
227	Two-dimensional semiconducting Cs(<scp>i</scp>)/Bi(<scp>iii</scp>) bimetallic iodide hybrids for light detection. Materials Chemistry Frontiers, 2021, 5, 973-978.	5.9	4
228	Smooth and mechanically robust random metallic mesh electrode modified by thermally transferred PEDOT: PSS for ITO-Free flexible organic light-emitting diodes. Organic Electronics, 2022, , 106498.	2.6	4
229	White organic light-emitting devices fabricated by spin-coating molecular materials. Science Bulletin, 2010, 55, 986-991.	1.7	3
230	Theoretical study of density-dependent intraexcitonic transitions in optically excited quantum wells. Journal of Physics Condensed Matter, 2011, 23, 345801.	1.8	3
231	Optimizing biased semiconductor superlattices for terahertz amplification. Applied Physics Letters, 2014, 105, 062112.	3.3	3
232	Charge Transport between Coupling Colloidal Perovskite Quantum Dots Assisted by Functional Conjugated Ligands. Angewandte Chemie, 2018, 130, 5856-5860.	2.0	3
233	Dibenzo[<i>f</i> , <i>h</i>]furo[2,3- <i>b</i>]quinoxaline-based molecular scaffolds as deep blue fluorescence materials for organic light-emitting diodes. New Journal of Chemistry, 2021, 46, 419-425.	2.8	3
234	Harvesting the Triplet Excitons of Quasi-Two-Dimensional Perovskite toward Highly Efficient White Light-Emitting Diodes. Journal of Physical Chemistry Letters, 2022, 13, 3674-3681.	4.6	3

#	Article	IF	CITATIONS
235	Semiconductivity and high stability in centimetric two-dimensional bismuth–silver hybrid double perovskites. Materials Chemistry Frontiers, 2022, 6, 2135-2142.	5.9	3
236	Investigation on the escaped and trapped emission in organic light-emitting devices. Optics Communications, 2012, 285, 1625-1630.	2.1	2
237	Deciphering perovskite crystal growth in interdiffusion protocol for planar heterojunction photovoltaic devices. Organic Electronics, 2018, 53, 88-95.	2.6	2
238	A cation-regulation strategy for achieving high-performance perovskite solar cells via a fully-evaporation process. Organic Electronics, 2020, 82, 105710.	2.6	2
239	Mono-, di- and tri-nuclear Pt ^{II} (C^N)(N-donor ligand)Cl complexes showing aggregation-induced phosphorescent emission (AIPE) behavior for efficient solution-processed organic light-emitting devices. Materials Chemistry Frontiers, 2021, 5, 4160-4173.	5.9	2
240	Cohesively Enhancing the Conductance, Mechanical Robustness, and Environmental Stability of Random Metallic Mesh Electrodes via Hot-Pressing-Induced In-Plane Configuration. ACS Applied Materials & Interfaces, 2021, 13, 41836-41845.	8.0	2
241	Ultra-thick inverted green organic light-emitting diodes for high power efficiency over 300 lm/W. Organic Electronics, 2022, 101, 106414.	2.6	2
242	Hole Transport Layer Free Perovskite Light-Emitting Diodes With High-Brightness and Air-Stability Based on Solution-Processed CsPbBr3-Cs4PbBr6 Composites Films. Frontiers in Chemistry, 2022, 10, 828322.	3.6	2
243	Bright and efficient sky-blue perovskite light-emitting diodes via doping of π-conjugated molecule tetraphenylethylene. Órganic Electronics, 2022, 102, 106441.	2.6	2
244	Ternary Halogen Doping for Efficient and Stable Airâ€Processed Allâ€Inorganic Perovskite Solar Cells. Solar Rrl, 0, , .	5.8	2
245	Comment on "Surface plasmon coupled electroluminescent emission―[Appl. Phys. Lett. 92, 103304 (2008)]. Applied Physics Letters, 2008, 93, 266101.	3.3	1
246	A tris(8-hydroxyquinoline) aluminum-based organic bistable device using ITO surfaces modified by Ag nanoparticles. Journal Physics D: Applied Physics, 2013, 46, 445107.	2.8	1
247	Electroluminescence of solution-processed organic light-emitting diodes based on fluorescent small molecules and polymer as hole-transporting layer. Physica Status Solidi (A) Applications and Materials Science, 2013, 210, 2556-2560.	1.8	1
248	An ultra-thin inorganic interlayer strategy for achieving efficient inverted planar perovskite solar cells and modules with high fill factor. Organic Electronics, 2020, 87, 105937.	2.6	1
249	å^†å构型å⁻¹æœ‰æœºåŠå⁻¼ä¼2"å^†åTPD, DDBå'ŒNPBæ;€å°"性能的影哕 Scientia Sinica Chimica, 2	01 3).4 3, 4	93±501.
250	Stable two-dimensional lead iodide hybrid materials for light detection and broadband photoluminescence. Materials Chemistry Frontiers, 2021, 6, 71-77.	5.9	1
251	Interaction between subpicosecond laser and fused silica. , 2005, 5646, 224.		Ο
252	Investigation on the parameters of dense electronic plasma induced by femtosecond laser in fused silica. Springer Series in Chemical Physics, 2005, , 354-356.	0.2	0

#	Article	IF	CITATIONS
253	The escaped and trapped emission in organic light-emitting devices. , 2010, , .		0
254	Optimal design and experimental realization of DBR-metal microcavity organic lasers. Proceedings of SPIE, 2010, , .	0.8	0
255	One-pot synthesis of stabilizer-free Ag-Graphene Nanocomposite and its potential application on photodegradation of RhB. , 2013, , .		0
256	Formation of charge-transfer complex and enlarging the absorption ability of MEH-PPV by Ag-Graphene Nanocomposite. , 2013, , .		0
257	Silver nanowires effect on photoluminescence of ZnO films deposited on different substrates with graphene oxide paper. , 2014, , .		0
258	Realization of white organic light-emitting devices using single green emitter by coupled microcavities with two modes. Applied Physics Express, 2015, 8, 022103.	2.4	0
259	Fabrication of microtapered/helical long-period fiber gratings with a CO <inf>2</inf> laser fusion splicer. , 2017, , .		0
260	Novel Long-Period Fiber Gratings: Fabrication and Sensing Applications. , 2017, , .		0
261	Simulation and optimization for the optical performance of top-emitting OLED. , 2017, , .		0